International Journal of Earth Sciences Knowledge and Applications
journal homepage: http://www.ijeska.com/index.php/ijeska
e-ISSN: 2687-5993

Research Article https://doi.org/10.5281/zenodo.22164814

Hydrothermal Alteration and Mineralization of the Gujareti Ore Occurrence (Achara–Trialeti Fold-and-Thrust Belt, Georgia)

Giorgi Mindiashvili[1]*, David Bluashvili[2], Tornike Lipartia[2], Nino Jafaridze[2], Keti Benashvili[2], Vakhtang Bluashvili[2], Meri Lekishvili[2]

[1]*Ivane Javakhishvili Tbilisi State University, Tbilisi, Georgia*
[2]*Georgian Technical University, Tbilisi, Georgia*

INFORMATION

Article history
Received 15 July 2026
Accepted 29 August 2026
Published 31 August 2026

Contact
*Giorgi Mindiashvili
giorgim1994@gmail.com (GM)

How cite
Mindiashvili, G., Bluashvili, D., Lipartia, T., Jafaridze, N., Benashvili, K., Bluashvili, V., Lekishvili, M., 2026. Hydrothermal Alteration and Mineralization of the Gujareti Ore Occurrence (Achara–Trialeti Fold-and-Thrust Belt, Georgia). *International Journal of Earth Sciences Knowledge and Applications* 8 (2), 223–231. https://doi.org/10.5281/zenodo.22164814 .

Abstract
Hydrothermal alteration plays a fundamental role in understanding ore-forming processes and improving mineral exploration. This study presents an integrated characterization of the Gujareti hydrothermal system (Achara–Trialeti Fold-and-Thrust Belt, Georgia) using ASTER remote sensing, petrographic and ore microscopic observations, X-ray diffraction (XRD), and whole-rock X-ray fluorescence (XRF) geochemistry. Satellite-derived alteration mapping identified three principal alteration domains, including silica-enriched, mica-rich, and carbonatized zones, which exhibit a close spatial association with structurally controlled mineralization. Petrographic and XRD analyses indicate that the alteration assemblage is dominated by quartz and sericite with localized alunite and calcite, whereas ore microscopy reveals pyrite as the principal sulfide, accompanied by chalcopyrite, sphalerite, minor galena, and microscopic native gold. Geochemical discrimination diagrams consistently indicate extensive silicification, alkali depletion, and progressive feldspar alteration, reflecting a well-developed hydrothermal alteration system. The strong agreement between remote sensing, mineralogical, and geochemical datasets demonstrates that integrating multiple analytical techniques substantially improves the recognition of alteration patterns and their relationship to mineralization. The proposed multidisciplinary workflow provides a reliable approach for reconstructing hydrothermal evolution and represents an effective exploration strategy applicable to volcanic-hosted hydrothermal systems in the Lesser Caucasus and comparable metallogenic provinces.

Keywords
Hydrothermal alteration, Ore microscopy, Remote sensing, Gujareti, Achara–Trialeti Fold-and-Thrust Belt, Georgia

1. Introduction

Hydrothermal alteration is a fundamental component of ore-forming systems because it records fluid–rock interaction and provides information on the evolution and spatial organization of mineralizing processes. Alteration mineral assemblages reflect variations in fluid composition, temperature, pH, host-rock composition, and water–rock interaction, and their identification is therefore important both for reconstructing hydrothermal systems and for mineral exploration (Reed, 1997; Hedenquist et al., 2000; Pirajno, 2009).

In volcanic-hosted hydrothermal environments, alteration commonly develops as spatially organized mineral assemblages controlled by fluid chemistry, permeability, lithology, and structural architecture. Silicification, sericitization, argillic alteration, carbonatization, and propylitic alteration are among the principal alteration styles associated with porphyry and epithermal systems. Their spatial distribution and mineralogical relationships can provide important constraints on fluid pathways, alteration evolution, and the location of mineralized zones (Hedenquist et al., 2000; Pirajno, 2009; Sillitoe, 2010).

Remote sensing has considerably expanded the ability to map hydrothermal alteration over large and relatively inaccessible areas. In particular, the Advanced Spaceborne Thermal Emission and Reflection Radiometer (ASTER) is widely used to discriminate spectrally responsive alteration minerals and mineral groups because of diagnostic absorption features in the short-wave infrared (SWIR) region (Yamaguchi et al., 1998; Rowan and Mars, 2003; Mars and Rowan, 2006). ASTER-based approaches have also been applied in southern Georgia, including the Gujareti–Khachkovi ore field and the Bektakari–Bneli Khevi ore knot, demonstrating their potential for regional recognition of hydrothermal alteration patterns (Mindiashvili et al., 2023; Mindiashvili et al., 2024). However, satellite-derived spectral anomalies are indirect expressions of surface mineralogy and, when considered independently, do not necessarily establish their mineralogical origin or their relationship to mineralization.

Ground-based mineralogical, petrographic, and geochemical observations are therefore necessary to evaluate the geological significance of remotely detected alteration patterns. Petrography provides information on alteration textures and replacement relationships, reflected-light microscopy constrains sulfide assemblages and relative mineral-forming sequences, X-ray diffraction (XRD) identifies alteration mineral assemblages, and whole-rock geochemistry records elemental redistribution associated with fluid–rock interaction (Rollinson, 1993; Deer et al., 2013). Integration of these datasets can therefore test whether remotely mapped alteration domains correspond to mineralogically and geochemically expressed hydrothermal processes rather than simply to variations in primary lithology or surface spectral response.

The Achara–Trialeti Fold-and-Thrust Belt is one of the principal metallogenic provinces of the Lesser Caucasus and contains numerous hydrothermal mineral occurrences hosted by Eocene volcanic and subvolcanic rocks (Adamia et al., 2011). Previous investigations of the Dzama–Gudjareti ore knot and the Gujareti–Khachkovi ore field have established the regional geological, metallogenic, structural, geophysical, and remote-sensing framework and have demonstrated the exploration potential of the area (Bluashvili et al., 2020; Bluashvili and Mindiashvili, 2021; Mindiashvili et al., 2022; Mindiashvili et al., 2023; Mindiashvili et al., 2024). Nevertheless, at the scale of the Gujareti ore occurrence, the mineralogical and geochemical significance of the remotely detected alteration patterns and their relationship to sulfide mineralization have remained insufficiently constrained. In particular, it has not been established whether the spatially mapped alteration anomalies correspond to ground-verified alteration mineral assemblages and systematic geochemical modification of the volcanic host rocks. This limits interpretation of the internal alteration architecture of the Gujareti hydrothermal system and its relationship to mineralization.

The present study addresses this problem by examining the spatial, mineralogical, petrographic, and geochemical expressions of hydrothermal alteration within the Gujareti ore occurrence. The results establish a spatial association between the principal mineralized sector and overlapping silica and mica-related alteration anomalies, while ground-based observations document quartz–sericite-dominated alteration with localized alunite and calcite, together with pyrite-dominated sulfide mineralization containing subordinate chalcopyrite and sphalerite. Whole-rock geochemical patterns further indicate pronounced alkali redistribution, including Na depletion and relative K–Al enrichment, consistent with feldspar destruction and sericitic alteration. The principal contribution of this study is therefore not simply the combination of several analytical techniques, but the demonstration that alteration patterns detected at satellite scale correspond to mineralogical, textural, and geochemical expressions of hydrothermal alteration and are spatially associated with the mineralized part of the Gujareti system.

These relationships are also relevant beyond Gujareti because distinguishing hydrothermal alteration from lithologically controlled spectral variability is a recurring challenge in remote-sensing-based exploration of volcanic terranes. The Gujareti example demonstrates how satellite-scale alteration patterns can be evaluated against independent mineralogical and geochemical observations to constrain the geological significance of surface anomalies and their relationship to structurally controlled mineralization. Accordingly, the objective of this study is to characterize the spatial distribution, mineral assemblages, geochemical evolution, and mineralization relationships of hydrothermal alteration at Gujareti and to evaluate the consistency of these features across remote-sensing and ground-based datasets.

2. Geological Background

The Gujareti ore occurrence is situated within the central part of the Achara–Trialeti Fold-and-Thrust Belt, which represents one of the principal metallogenic provinces of the Lesser Caucasus. The belt formed during the Late Cretaceous–Cenozoic evolution of the Neo-Tethyan domain and is characterized by extensive volcanic, volcaniclastic, and intrusive complexes generated during subduction-related magmatism and subsequent tectonic evolution (Adamia et al., 2011; Gamkrelidze, 1986).

The investigated area is composed predominantly of Middle Eocene volcanic and volcaniclastic rocks belonging to the Dviri Suite. These rocks consist mainly of basaltic andesites, andesites, volcanic breccias, tuffs, and tuff-breccias, which constitute the principal host rocks for hydrothermal alteration and ore mineralization. The volcanic sequence is locally intruded by intermediate subvolcanic bodies that are spatially associated with mineralized structures (Bluashvili et al., 2020; Mindiashvili et al., 2022).

Structurally, the ore occurrence is controlled by a dense network of regional and local faults. The dominant fault systems trend NW–SE, NE–SW, and E–W, producing a complex fracture network that acted as the principal pathway for hydrothermal fluids. Mineralization is preferentially concentrated along fault intersections and highly fractured zones, where permeability was significantly enhanced (Bluashvili et al., 2020; Mindiashvili et al., 2024).

Hydrothermal alteration is widespread throughout the investigated area and is closely associated with the major structural corridors. Remote sensing analysis reveals extensive silica-enriched zones accompanied by localized mica-rich and carbonate-altered domains. The coincidence of these alteration anomalies with mapped fault systems indicates strong structural control on hydrothermal fluid circulation (Mindiashvili et al., 2023; Mindiashvili et al., 2024).

The schematic geological map (Fig. 1) shows that the Gujareti occurrence comprises several hydrothermally altered bodies developed within the volcanic succession. Silicified zones represent the dominant alteration type and are spatially associated with disseminated and vein-type sulfide mineralization. Carbonate alteration occurs locally, whereas mica-rich alteration develops mainly adjacent to the silicified domains.

Ore mineralization is dominated by pyrite, accompanied by subordinate chalcopyrite, sphalerite, and minor galena, while native gold occurs as fine inclusions within sulfide minerals. The distribution of sulfide mineralization closely follows the principal fault zones and silicified bodies, indicating that structural permeability played a fundamental role in ore deposition (Bluashvili and Mindiashvili, 2021; Mindiashvili et al., 2022).

The geological, structural, and alteration characteristics indicate that the Gujareti occurrence represents a structurally controlled hydrothermal system developed within an Eocene volcanic arc environment. The close spatial association between regional faulting, pervasive silicification, sericitization, sulfide mineralization, and intermediate magmatism demonstrates that hydrothermal activity was focused along long-lived tectonic structures that controlled both fluid migration and ore precipitation (Sillitoe, 2010; Pirajno, 2009).

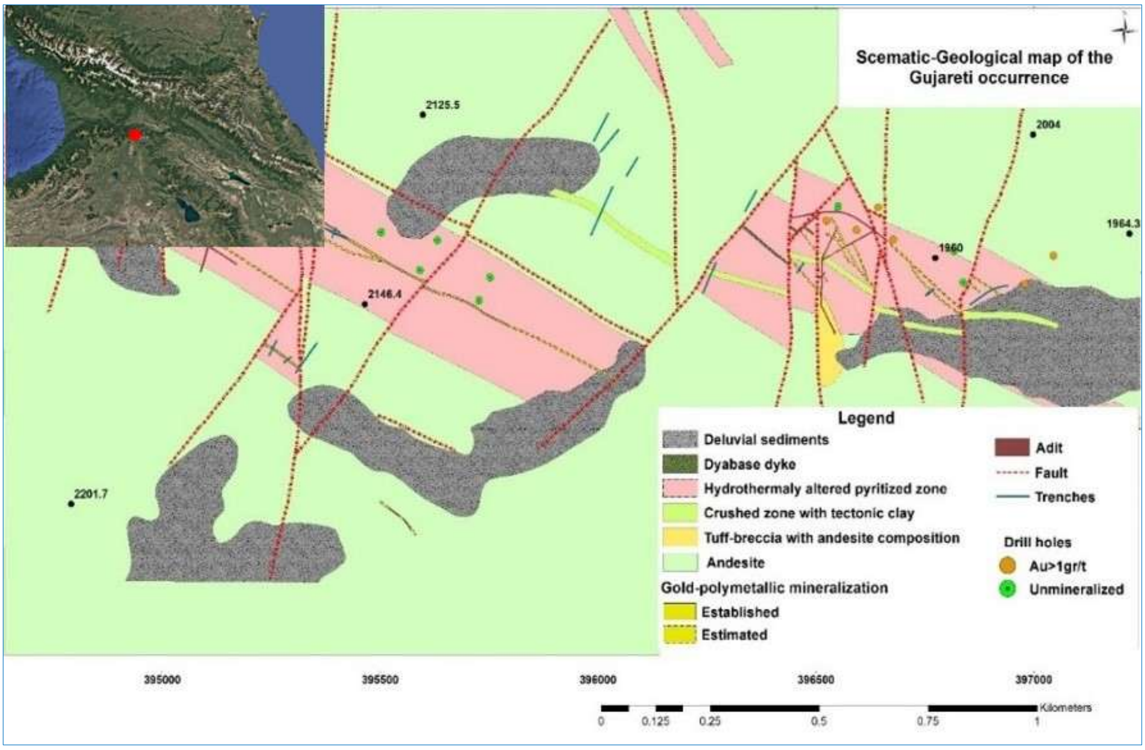

Fig. 1. Location and schematic geological map of the Gujareti ore occurrence, showing the distribution of hydrothermally altered zones, fault systems, lithological units, and mineralized structures by M. Tskhelishvili

3. Materials and Methods

3.1. Remote Sensing Analysis of Hydrothermal Alteration

Hydrothermal alteration mapping was performed using multispectral ASTER (Advanced Spaceborne Thermal Emission and Reflection Radiometer) satellite imagery. ASTER data were selected because of their sensitivity to diagnostic spectral absorption features of hydroxyl-bearing, carbonate, and silica-rich minerals commonly associated with hydrothermal alteration (Yamaguchi et al., 1998; Rowan and Mars, 2003; Mars and Rowan, 2006).

The satellite data were processed within the QGIS environment, where spectral enhancement techniques were applied to delineate alteration anomalies. Image processing and spatial analysis enabled discrimination of silica-enriched, carbonatized, and mica-rich zones throughout the study area. The resulting alteration maps were integrated with geological observations to evaluate the spatial relationship between hydrothermal alteration and mineralization.

3.2. Petrographic and Ore Microscopic Investigations

Representative samples were prepared as polished thin sections for petrographic and microscopic investigation. Microscopic investigations were carried out at the Karlsruhe Institute of Technology (KIT), Germany. Petrographic observations were performed using an Olympus polarizing microscope under plane-polarized light (PPL) and cross-polarized light (XPL). Mineral identification was based on optical properties, including crystal habit, relief, cleavage, pleochroism, twinning, extinction characteristics, and interference colours. Reflected-light microscopy was used to characterize ore mineral assemblages, textural relationships, replacement features, and fracture-controlled sulfide mineralization.

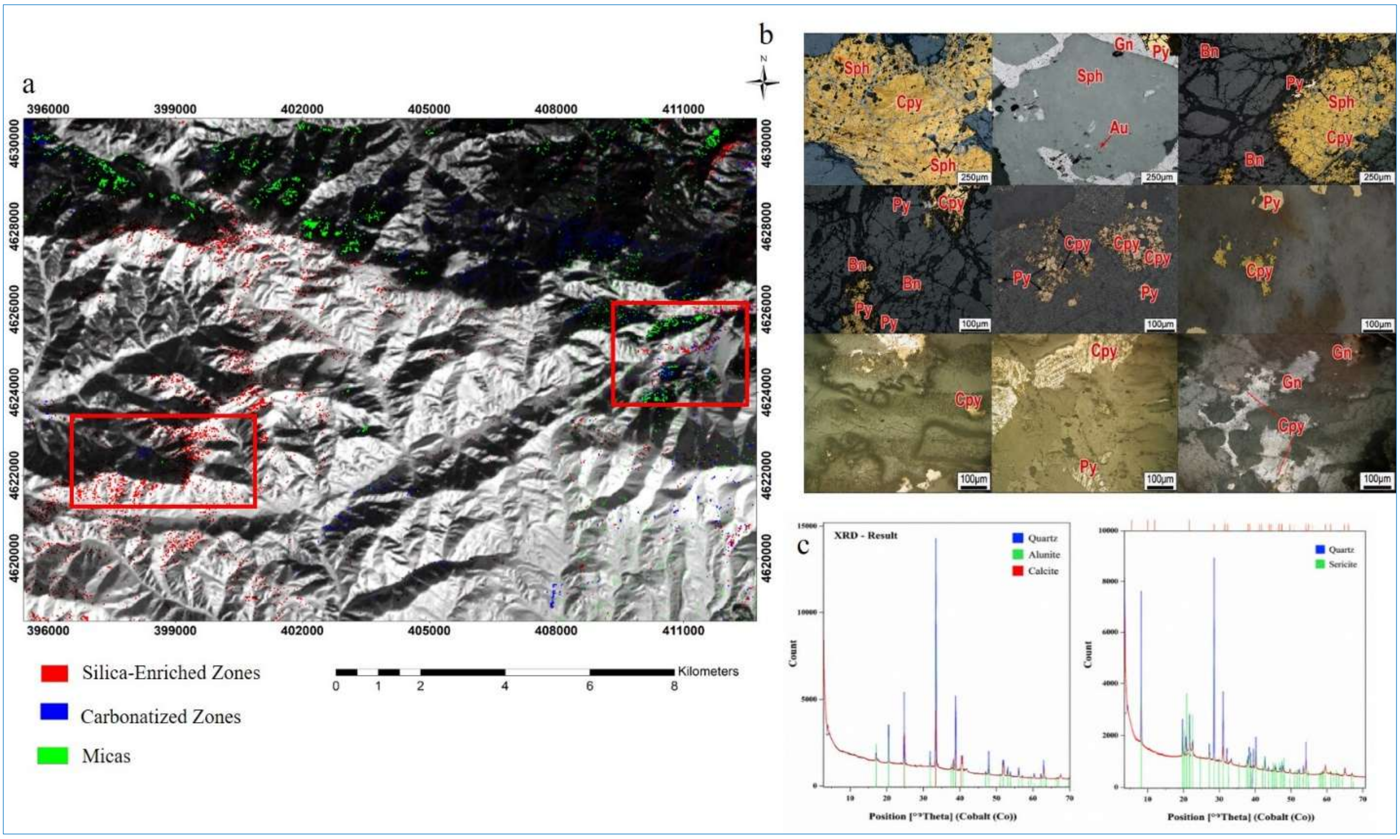

Fig. 2. Spatial distribution of hydrothermal alteration zones derived from ASTER imagery, together with representative ore microscopy images and XRD diffractograms from the Gujareti ore occurrence

3.3. X-ray Fluorescence Geochemical Analysis

Whole-rock X-ray fluorescence (XRF) analyses were performed on all 55 hydrothermally altered rock samples. The analytical work was carried out at the Department of Applied Geology, Georgian Technical University, and the Alexander Janelidze Institute of Geology, Georgia. XRF analysis was used to determine whole-rock elemental compositions to characterize hydrothermal alteration and to construct the geochemical discrimination diagrams used in this study.

3.4. X-ray Diffraction Analysis

X-ray diffraction (XRD) analysis was performed on 12 representative samples selected from the 55 hydrothermally altered rock samples collected from the Gujareti ore occurrence. The analyzed samples were selected to represent the different types of hydrothermal alteration encountered during field sampling. XRD analyses were carried out at the Alexander Tvalchrelidze Caucasian Institute of Mineral Resources, Georgia. The diffraction patterns were used to determine the mineralogical composition of the hydrothermally altered rocks and to identify the principal alteration minerals, including quartz, sericite, alunite, and calcite. The XRD results were subsequently compared with petrographic observations and whole-rock geochemical data to evaluate the mineralogical expression of hydrothermal alteration within the Gujareti hydrothermal system.

3.5. Geochemical Data Processing and Alteration Discrimination

The XRF dataset was processed using ioGAS software and the Python programming language. Major-element concentrations were recalculated into molar proportions where necessary, and several established hydrothermal alteration discrimination diagrams were constructed to evaluate alteration intensity, elemental mobility, and mineralogical evolution.

The following diagrams were employed:

- Al–K–Mg ternary diagram to distinguish advanced argillic, phyllic, potassic, and least-altered assemblages.
- Fe oxide–Quartz–Kaolinite diagram to evaluate silicification, ferruginization, and kaolinization.
- K/Rb–Al diagram to characterize aluminium enrichment and clay–muscovite alteration.
- Na/Al versus K/Al molar ratio diagram (after Davies and Whitehead, 2006) to assess feldspar destruction, sodium depletion, and potassium metasomatism.
- Phyllite ferruginisation diagram (after Jeffcoate et al., 2013) to evaluate iron mobility during hydrothermal alteration.
- Volcanic rock alteration diagram to investigate the geochemical evolution of volcanic rocks during hydrothermal alteration.

The final interpretation of the hydrothermal system was based on the integration of ASTER remote sensing, petrographic observations, microscopy, XRD mineralogical analyses, and XRF geochemical data. Spatial analysis was conducted using QGIS, geochemical visualization was performed in ioGAS, and additional calculations and graphical processing were carried out in Python. This integrated workflow enabled characterization of the spatial distribution of hydrothermal alteration, mineral assemblages, alteration mineralogy, and the geochemical evolution of the investigated hydrothermal system.

4. Results

4.1. Spatial Distribution of Hydrothermal Alteration

Remote sensing analysis revealed three principal hydrothermal alteration domains within the investigated area (Fig. 2a). Silica-enriched zones constitute the most extensive alteration pattern and occur predominantly along linear and structurally controlled corridors. Carbonatized zones are considerably less abundant and are spatially restricted, whereas mica-enriched zones are concentrated within discrete clusters closely associated with the silica anomalies.

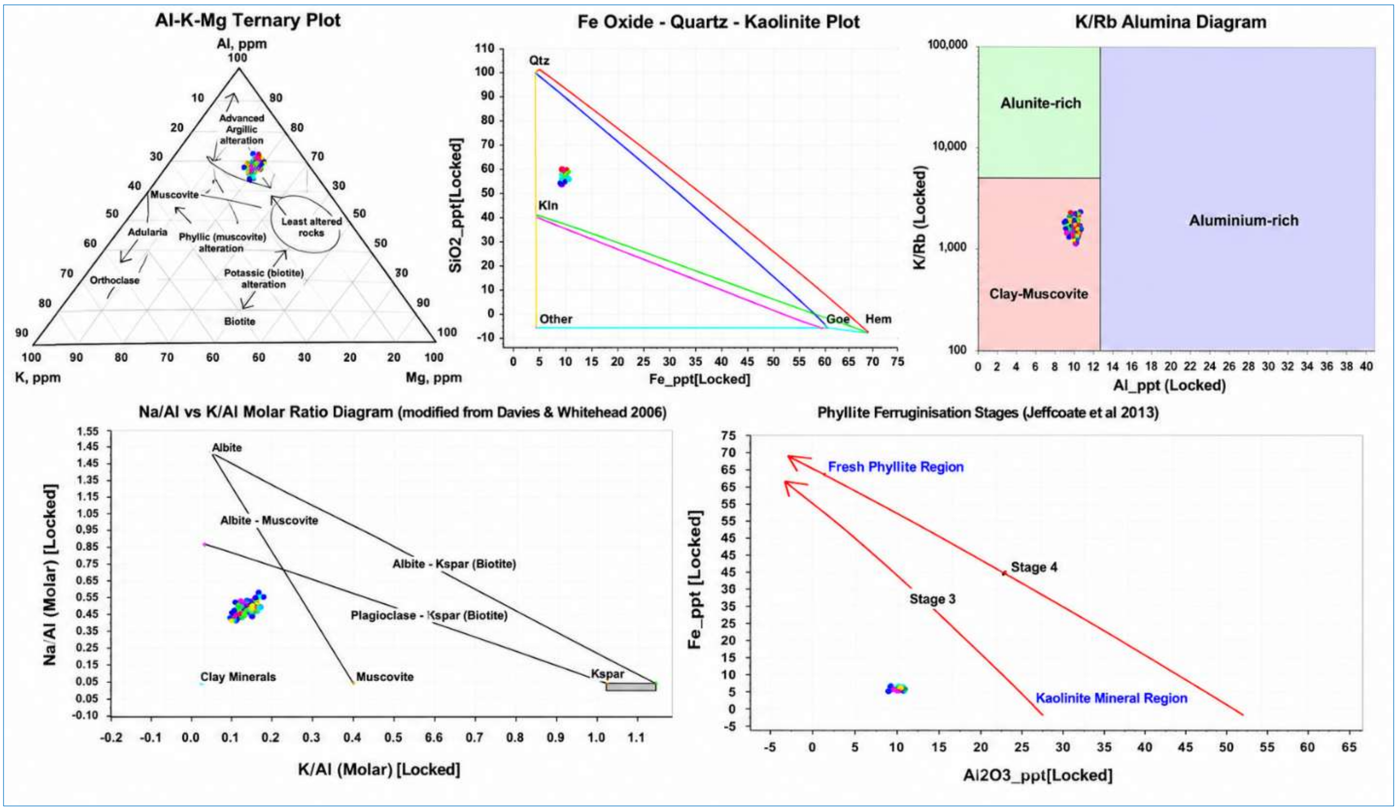

Fig. 3. Integrated geochemical discrimination diagrams based on whole-rock XRF analyses showing the principal hydrothermal alteration trends within the Gujareti ore occurrence

The highest density of overlapping silica and mica anomalies is observed within the central-eastern part of the study area, where the investigated mineral occurrence is located. This spatial relationship indicates that the mineralized zone coincides with the most intensely hydrothermally altered sector identified from satellite-derived alteration mapping.

Ore microscopy demonstrates that sulfide mineralization is dominated by pyrite, accompanied by subordinate chalcopyrite and sphalerite, whereas galena occurs locally in minor quantities (Fig. 2b).

Pyrite occurs as euhedral to subhedral crystals and also as disseminated and vein-related aggregates. Chalcopyrite is commonly developed along fractures and grain boundaries of pyrite or occupies interstitial positions between pyrite crystals. Sphalerite is closely associated with chalcopyrite and locally forms composite intergrowths with both chalcopyrite and pyrite. Minor galena is observed as isolated grains associated with sphalerite.

Fine, highly reflective microscopic inclusions were observed within chalcopyrite and sphalerite and are tentatively interpreted as native gold based on their reflected-light optical characteristics. Because these inclusions have not been independently verified by microanalytical techniques such as SEM–EDS or EPMA, their identification as native gold should be regarded as preliminary. Their textural association with chalcopyrite and sphalerite suggests that the observed inclusions may be related to the later Cu–Zn sulfide assemblage; however, their precise paragenetic position cannot be conclusively established from reflected-light microscopy alone.

4.2. Mineralogical Composition (XRD)

X-ray diffraction analyses indicate that quartz is the dominant mineral across the samples analyzed (Fig. 2c). The diffraction patterns also identify sericite, alunite, and calcite.

Quartz produces the strongest diffraction peaks in all analyzed spectra, demonstrating pervasive silicification. Sericite is consistently present in altered samples, whereas alunite occurs locally, indicating zones affected by advanced hydrothermal alteration. Calcite is restricted to specific samples and reflects localized carbonate alteration.

The XRD results therefore confirm the coexistence of silicification, sericitization, advanced argillic alteration, and localized carbonatization within the investigated hydrothermal system.

4.3. Geochemical characteristics of alteration (Fig.3)

4.3.1. Al–K–Mg Ternary Diagram

Samples plot almost within the Advanced Argillic Alteration field. None of the analyzed samples fall within the least altered, propylitic, or potassic alteration fields. The clustering indicates strong enrichment in Al relative to Mg and partial depletion of K.

4.3.2. Fe oxide–Quartz–Kaolinite Diagram

All analytical points occupy a narrow cluster between the quartz and kaolinite end-members. Their position indicates silica-rich compositions accompanied by kaolinite enrichment, whereas Fe-oxide contents remain comparatively low.

4.3.3. K/Rb–Al Diagram

The analyzed samples cluster within the Clay–Muscovite field near the boundary with the aluminium-rich domain. The limited scatter suggests relatively uniform hydrothermal alteration affecting the investigated rocks.

4.3.4. Na/Al versus K/Al Molar Ratios

The Na/Al–K/Al plot shows that all samples occupy a restricted area along the compositional trend between plagioclase and muscovite. The distribution reflects significant depletion of Na accompanied by relative enrichment in K and Al.

4.3.5. Phyllite Ferruginisation Diagram

Samples are concentrated within the Kaolinite Mineral Region, well outside the ferruginization trends. Iron enrichment is therefore limited, whereas kaolinite-related alteration dominates the analyzed assemblage.

The mineralogical, petrographic, and geochemical datasets consistently indicate that the investigated hydrothermal system is characterized by: pervasive silicification; widespread sericitization; localized alunitization; localized carbonatization; limited ferruginization; abundant pyrite accompanied by chalcopyrite and sphalerite; native gold hosted mainly within later sulfide assemblages.

Spatial coincidence between remotely sensed silica- and mica-enriched zones, sulfide mineralization observed in ore microscopy, and quartz–sericite–alunite assemblages identified by XRD demonstrates that the central mineralized sector corresponds to the most intensely hydrothermally altered part of the investigated area.

5. Discussion

The integration of ASTER remote sensing, petrographic observations, XRD mineral identification, and whole-rock XRF geochemistry provides a coherent picture of the hydrothermal alteration developed within the Gujareti ore occurrence. Although each dataset represents a different observational scale, their spatial and mineralogical agreement suggests that they record different aspects of the same hydrothermal system. The ASTER-derived alteration map indicates that silica-enriched zones constitute the most extensive alteration domains within the investigated area. These anomalies are preferentially developed along major structural corridors and coincide with the mapped mineral occurrence. While satellite-derived anomalies alone cannot unequivocally distinguish hydrothermal quartz from other silica-bearing lithologies, their spatial coincidence with sulfide mineralization, sericitic alteration, and XRD-confirmed quartz-rich assemblages strongly suggests that the detected silica anomalies largely reflect hydrothermal silicification rather than primary lithological variations (Pirajno, 2009; Hedenquist et al., 2000).

The distribution of mica-rich anomalies is considerably more restricted and mainly confined to the central part of the hydrothermal system. This spatial relationship may indicate that potassium-bearing alteration minerals developed preferentially in zones where hydrothermal fluids interacted more intensively with feldspar-bearing volcanic rocks. Such a pattern is compatible with localized sericitization superimposed upon more extensive silicification.

Carbonate anomalies occupy only limited areas compared with silica alteration. This observation may suggest that carbonatization represented a relatively localized alteration event or developed only under specific physicochemical conditions during hydrothermal evolution. The restricted distribution of carbonate minerals also implies that carbonate precipitation was probably not the dominant fluid-buffering mechanism throughout the system.

Overall, the alteration map suggests that hydrothermal activity was spatially heterogeneous and structurally controlled, with silicification representing the dominant alteration process and mica-rich alteration developing within its central portions.

Petrographic observations reveal that hydrothermal alteration affected both the volcanic groundmass and primary phenocrysts to varying degrees. Plagioclase commonly exhibits partial to nearly complete replacement by fine-grained sericite, whereas pyroxene and amphibole locally preserve relict crystal cores surrounded by alteration products. Such textural relationships are consistent with progressive fluid-rock interaction rather than instantaneous mineral replacement.

Quartz occurs both as primary volcanic material and as secondary hydrothermal quartz. Secondary quartz commonly fills fractures, replaces primary minerals, or occurs as fine-grained recrystallized aggregates. These observations agree well with the extensive silica anomalies identified by ASTER imagery and with the dominant quartz reflections detected by XRD analyses.

The occurrence of sericite together with locally identified alunite is particularly significant. These minerals generally form under different fluid conditions, and their coexistence may indicate temporal or spatial variations in fluid acidity. Rather than representing a single homogeneous alteration event, the observed assemblages may therefore record successive hydrothermal pulses characterized by evolving fluid composition.

Although the mineral assemblages resemble those reported from volcanic-hosted magmatic-hydrothermal systems elsewhere, the available data do not allow precise reconstruction of fluid composition or temperature. Nevertheless, the observed alteration textures strongly support prolonged hydrothermal overprinting of the volcanic sequence.

The major-element geochemical data further support petrographic observations and indicate systematic redistribution of mobile elements during alteration.

The Al–K–Mg ternary diagram places most samples within or close to the advanced argillic alteration field. This distribution may reflect substantial depletion of magnesium accompanied by relative enrichment of aluminium. Magnesium is commonly removed during alteration of ferromagnesian minerals, whereas aluminium tends to remain relatively immobile and becomes concentrated in secondary aluminosilicate minerals. Although this interpretation is consistent with the observed mineral assemblages, it should be noted that major-element compositions may also be influenced by the primary composition of the host rocks (Sillitoe, 2010).

The Na/Al versus K/Al molar ratio diagram indicates pronounced sodium depletion relative to potassium. Such geochemical behaviour is compatible with destruction of plagioclase and progressive replacement by sericite. Petrographic observations showing extensive sericitization of feldspar phenocrysts provide independent support for this interpretation.

Similarly, the K/Rb–Al diagram places most samples within the clay–muscovite field. Because rubidium readily substitutes for potassium within white mica, this distribution suggests that potassium-bearing phyllosilicates represent an important component of the alteration assemblage. The agreement between geochemical discrimination diagrams, XRD mineralogy, and microscopic observations considerably increases confidence in this interpretation.

The Fe oxide–Quartz–Kaolinite diagram shows that most samples cluster closer to the quartz-rich part of the diagram than to the iron oxide end-member. This distribution may indicate that silica addition was more important than extensive iron oxidation during alteration. Such an interpretation is also compatible with the relatively limited abundance of secondary hematite and goethite observed petrographically.

Collectively, the geochemical diagrams consistently indicate extensive alkali redistribution, relative aluminium enrichment, and widespread silicification. Although these diagrams cannot uniquely determine alteration conditions, their mutual agreement with mineralogical observations suggests that they successfully capture the dominant geochemical processes operating during hydrothermal alteration.

Ore microscopy reveals a sulfide assemblage dominated by pyrite with subordinate chalcopyrite and sphalerite. Pyrite commonly forms euhedral to subhedral crystals, whereas chalcopyrite occurs along fractures and grain boundaries within pyrite, suggesting that Cu-bearing mineralization postdated at least part of the main pyrite-forming stage. Sphalerite locally forms intergrowths with chalcopyrite, indicating a close textural relationship between Cu- and Zn-bearing sulfides.

Fine, highly reflective inclusions observed within chalcopyrite and sphalerite are tentatively interpreted as native gold based on their reflected-light optical characteristics. Their occurrence within the Cu–Zn sulfide assemblage may indicate a relationship with a relatively later stage of sulfide mineralization. However, because no SEM–EDS, EPMA, or comparable microanalytical verification was performed, both their identification as native gold and their precise paragenetic relationship should be considered preliminary. Further microanalytical investigation is required to confirm their composition and constrain the timing of possible gold deposition within the Gujareti hydrothermal system.

When considered together, the remote sensing, mineralogical, petrographic, and geochemical datasets suggest that the Gujareti hydrothermal system evolved through multiple stages rather than a single alteration event.

An early stage was probably characterized by extensive silica precipitation accompanied by widespread pyrite formation. Continued circulation of hydrothermal fluids appears to have promoted destruction of feldspars and development of sericitic alteration, as indicated by both petrographic observations and geochemical indices. Local occurrence of alunite may reflect later episodes of increased fluid acidity, although the available data do not permit reconstruction of the precise physicochemical evolution of the hydrothermal fluids.

The spatial coincidence between silica anomalies, structural lineaments, and sulfide mineralization further suggests that fault systems exerted an important control on hydrothermal fluid migration. Similar structural controls have also been recognized in nearby hydrothermal systems of the Gujareti–Khachkovi ore field, where integrated geophysical investigations demonstrated that hydrothermally altered sulfide-bearing zones are spatially associated with major fault zones, intrusive bodies, and fractured rocks (Bluashvili et al., 2024). Rather than representing isolated mineralized bodies, the observed alteration zones may therefore define interconnected pathways through which mineralizing fluids ascended.

The combined dataset does not unequivocally constrain the genetic classification of the hydrothermal system. Nevertheless, the observed association of extensive silicification, sericitization, localized advanced argillic alteration, and structurally controlled sulfide mineralization is broadly compatible with magmatic-hydrothermal systems developed in volcanic arc environments. Whether the Gujareti occurrence represents the upper expression of a porphyry-related system, an epithermal environment, or a transitional setting remains uncertain and require additional evidence, including fluid inclusion studies, stable isotope analyses, and detailed mineral chemistry.

From an exploration perspective, the results demonstrate the value of integrating satellite remote sensing with laboratory-based mineralogical and geochemical analyses. Individually, each method provides only partial information; however, their integration substantially improves confidence in the interpretation of hydrothermal alteration.

ASTER imagery efficiently delineated regional alteration patterns, whereas XRD confirmed the mineralogical composition of the detected anomalies. Petrographic and ore microscopic observations established the textural relationships between alteration minerals and sulfides, while XRF geochemistry quantified the elemental redistribution associated with hydrothermal processes. The convergence of these independent datasets suggests that the integrated workflow represents an effective approach for identifying prospective hydrothermal alteration zones and prioritizing targets for future exploration.

6. Conclusions

The Gujareti Ore Occurrence is characterized by a spatially heterogeneous, structurally controlled hydrothermal alteration system that developed within Middle Eocene volcanic rocks. ASTER-based mapping delineates extensive silica-enriched zones accompanied by more restricted mica-rich and carbonatized domains, with the strongest overlap of silica- and mica-related anomalies occurring within the principal mineralized sector. This spatial relationship indicates that the most prominent remotely detected alteration patterns coincide with the area of strongest hydrothermal modification and sulfide mineralization.

Mineralogical, petrographic, and geochemical observations show that silicification and sericitization are the dominant alteration processes at Gujareti. XRD analyses identify quartz and sericite as the principal alteration minerals, accompanied by localized alunite and calcite. Whole-rock geochemical patterns are characterized by silica-rich compositions, pronounced Na depletion, and relative K–Al enrichment, consistent with feldspar destruction and progressive sericitic alteration. Sulfide mineralization is dominated by pyrite, with subordinate chalcopyrite and sphalerite and minor galena. Textural relationships indicate that at least part of the Cu–Zn mineralization postdated the principal pyrite-forming stage. Fine, highly reflective inclusions observed within chalcopyrite and sphalerite are tentatively interpreted as native gold, although their composition and paragenetic significance require confirmation by microanalytical methods.

The spatial correspondence between ASTER-derived alteration anomalies, ground-verified mineral assemblages, whole-rock geochemical modification, and sulfide mineralization provides new constraints on the internal organization of the Gujareti Hydrothermal System. In particular, the concentration of silica- and mica-related alteration within the mineralized sector indicates that these alteration patterns can serve as useful indicators of structurally focused hydrothermal activity. The Gujareti case therefore provides a basis for evaluating remotely detected alteration anomalies in comparable volcanic-hosted hydrothermal systems of the Lesser Caucasus, while further fluid-inclusion, isotope, and mineral-chemical studies are required to more precisely constrain the genetic classification and physicochemical evolution of the system.

References

Adamia, S., Zakariadze, G., Chkhotua, T., Sadradze, N., Tsereteli, N., Chabukiani, A., Gventsadze, A., 2011. Geology of the Caucasus: A Review. Turkish Journal of Earth Sciences 20, 489-544. https://doi.org/10.3906/yer-1005-11.

Bluashvili, D., Benashvili, K., Mindiashvili, G., Makadze, M., 2024. Geophysical survey of the Khachovi gold-polymetallic ore occurrence (Adjara-Trialeti folded zone, Georgia). Baltica 37 (1), 66-76. https://doi.org/10.5200/baltica.2024.1.7.

Bluashvili, D., Benashvili, K., Mindiashvili, G., Makadze, D., 2020. New Data on the Dzama-Gudjareti Ore Knot (Georgia). Bulletin of the Georgian National Academy of Sciences 14 (3), 94-100.

Bluashvili, D., Mindiashvili, G., 2021. Noble Metals Potential of Gudjareti-Khachkovi Ore Field, Georgia. Engineering Advances 1 (2), 47-49. https://doi.org/10.26855/ea.2021.12.003.

Davies, J.F., Whitehead, R E., 2006. Alteration indices and mass changes associated with hydrothermal alteration of volcanic rocks. In: Geochemistry: Exploration, Environment, Analysis, 6 (3), 201-210.

Deer, W.A., Howie, R.A., Zussman, J., 2013. An Introduction to the Rock-Forming Minerals (3rd ed.). Mineralogical Society of Great Britain and Ireland.

Hedenquist, J.W., Arribas, A., Gonzalez-Urien, E., 2000. Exploration for Epithermal Gold Deposits. Reviews in Economic Geology 13, 245–277. https://doi.org/10.5382/Rev.13.07.

Jeffcoate, A.B., Harley, S.L., White, N.C., 2013. Geochemical discrimination of ferruginisation and hydrothermal alteration in metasedimentary rocks. Ore Geology Reviews 53, 84-98.

Mars, J.C., Rowan, L.C., 2006. Regional mapping of phyllic- and argillic-altered rocks in the Zagros magmatic arc, Iran, using Advanced Spaceborne Thermal Emission and Reflection Radiometer (ASTER) data and logical operator algorithms. Geosphere 2 (3), 161-186.

Mindiashvili, G., Benashvili, K., Makadze, D., Makadze, M., Bluashvili, V., Momtselidze, N., 2023. Remote Sensing Results of Gujareti-Khachkovi Ore Field (Adjara-Trialeti Folded Zone, Lesser Caucasus, Georgia). Bulletin of the Georgian National Academy of Sciences, 17 (1), 89-94.

Mindiashvili, G., Iobidze, G., Lipartia, T., Japaridze, N., Benashvili, K., Bluashvili, I., Kvirkvelia, M., Mekokishvili, D., Bluashvili, D., 2024. Identification of the data obtained by the remote sensing method within the Bektakari–Bnelikhevi ore knot. Mining Journal, 1 (47), 48-62. https://doi.org/10.36073/1512-407X/2024-48-62.

Mindiashvili, G., Bluashvili, D., Iobidze, G., Lipartia, T., Jafaridze, N., Benashvili, K., 2026. Application of machine learning to hydrothermal system analysis: Geochemical insights from the Bektakari–Bneli Khevi Ore Knot, Southern Georgia. Bulletin of the Mineral Research and Exploration 179, 107-123. https://doi.org/10.19111/bulletinofmre.1768420.

Mindiashvili, G., Bluashvili, D., Lipartia, T., Iobidze, G., Makadze, M., Jafaridze, N., Benashvili, K., Khetsuriani, G., Bluashvili, V., 2026. Magmatic-hydrothermal evolution and ore potential of the Bektakari–Bnelikhevi knot, Bolnisi ore district, the Lesser Caucasus. ANAS Transactions, Earth Sciences 1, 57-65. https://doi.org/10.33677/ggianas20260100166.

Pirajno, F., 2009. Hydrothermal Processes and Mineral Systems. Springer, Dordrecht.

Reed, M.H., 1997. Hydrothermal Alteration and its Relationship to Ore Fluid Composition. In: Geochemistry of Hydrothermal Ore Deposits (3rd ed.). John Wiley & Sons.

Rollinson, H.R., 1993. Using Geochemical Data: Evaluation, Presentation, Interpretation. Longman Scientific & Technical.

Rowan, L.C., Mars, J.C., 2003. Lithologic Mapping in the Mountain Pass, California Area Using Advanced Spaceborne Thermal Emission and Reflection Radiometer (ASTER) Data. Remote Sensing of Environment 84, 350-366. https://doi.org/10.1016/S0034-4257(02)00127-X.

Sillitoe, R.H., 2010. Porphyry Copper Systems. Economic Geology 105 (1), 3-41. https://doi.org/10.2113/gsecongeo.105.1.3.

Yamaguchi, Y., Kahle, A.B., Tsu, H., Kawakami, T., Pniel, M., 1998. Overview of Advanced Spaceborne Thermal Emission and Reflection Radiometer (ASTER). IEEE Transactions on Geoscience and Remote Sensing 36 (4), 1062-1071. https://doi.org/10.1109/36.700991.